EARTHQUAKE ENGINEERING AND STRUCTURAL DYNAMICS
Earthquake Engng. Struct. Dyn. **28**, 127–141 (1999)

OPTIMAL PLACEMENT OF DVFC CONTROLLERS ON BUILDINGS SUBJECTED TO EARTHQUAKE LOADING

MAKOLA M. ABDULLAH*,†

Department of Civil Engineering, Florida Agricultural and Mechanical University/Florida State University College of Engineering, Tallahassee, FL 32310, U.S.A.

SUMMARY

The dynamic responses of tall civil structures due to earthquakes are very important to the civil engineer. These dynamic responses can produce situations that can range from uncomfortable to unsafe for the building occupants. In recent years classical control theory has been used in civil engineering to reduce the dynamic responses of tall civil structures. Most optimal control algorithms for civil structures involve full state feedback control which requires good estimates of the velocity and displacements throughout the structure. However, there are several important advantages of output feedback control: it takes less computational effort and it has the robustness of passive systems. In this paper, optimal control algorithms are formulated for the optimization of feedback gains and controller placement for building structures. The fundamental basis for these algorithms is the calculation of the gradient of the performance function with respect to the gain matrix. The effectiveness of the algorithm is demonstrated for deterministic earthquake loads in the time domain. Copyright © 1999 John Wiley & Sons, Ltd.

KEY WORDS: optimal placement; tall buildings; earthquake design

INTRODUCTION

The destructive nature of earthquakes have always been important to the civil engineer. Even a relatively small earthquake can cause extensive structural damage and loss of life. Tall buildings are especially prone to structural damage due to earthquakes because of the large deflections of floors. There has been a tendency in some earthquake prone areas to use lighter materials and to impose height restrictions.[1] However, as structural engineering continues to advance, many of these restrictions are now being lifted. In recent years there have been numerous advances in earthquake building design as well as in active control technology that make it possible to build structures that will sustain deflections of much less magnitude than those built just twenty years ago.[2] Several of the active control techniques for controlling earthquakes include Active Tuned

* Correspondence to: Makola M. Abdullah, Department of Civil Engineering, Florida State University, Tallahassee, FL 32310-6046, U.S.A. E-mail: abdullah@eng.fsu.edu
† Assistant Professor

CCC 0098–8847/99/020127–15$17·50

Received 20 March 1998
Revised 1 July 1998

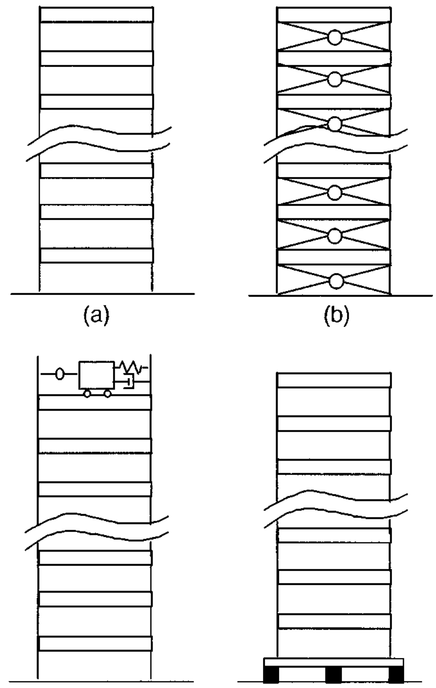

Figure 1. (a) Building with no control; (b) building with ATM; (c) building with an ATMD; (d) building with base isolation

Mass Dampers (ATMDs), Active Tendon Mechanisms (ATMs) and base isolation. Examples of these systems are shown in Figure 1.

Active tuned mass dampers are the most popular of all the control devices in use.[3–6] It is the most popular because they can be easily installed on existing structures. There are several commercial structures in Japan that employ this technology as well as buildings in New York and Boston. Tuned mass dampers, passive, active or semi -active, have been studied extensively as a way to mitigate the wind and earthquake response of tall buildings.[7,8] It is well known that the optimal place for an ATMD is on the top floor of a structure. Also, because of its bulky nature, it is not convenient to place an additional ATMD on any other floor. Because of this we will not study the placement of ATMDs. Base isolation systems consist of non-linear absorbers between the base of the structure and the ground. These absorbers allow the building to function as a single degree of freedom system.[9] The relative displacement between the base of the structure and the top can be greatly reduced. For tall buildings this method can produce very high overturning moments that can cause serious structural instabilities. The major disadvantage, however, is that this method cannot be realistically applied to existing structures. The Active Tendon Mechanism (ATM) gives much more flexibility in control.[10,11] Unlike ATMDs, it is possible to effect other modes rather than the fundamental mode. This can cause a greater reduction in the velocity and acceleration.

Direct Output Feedback Control (DOFC) as a means of controlling civil structures is a very new concept. Much of the literature that uses classical control theory in civil structures only mentions state feedback for use in controlling civil structures. It is extremely difficult to produce state feedback as that would require a large number of sensors and expensive computation times.[12] Output feedback control is the logical alternative because it produces control from a limited number of sensor outputs. Thus, with a limited number of sensors and actuators it can still be possible to produce effective control. DOFC is used to minimize the vibrations of buildings under earthquake loads, in the latter a form of DOFC was used called Direct Velocity Feedback Control (DVFC).[12] This method of control, for collocated sensor and actuator placement, is guaranteed to be stable.[13] This is a benefit for civil structures because of the uncertainty in earthquake and wind loading. The emphasis in both papers was the optimization of gains of ATMs.

Because active structural control is still a relatively new field, placement of controllers has not been extensively studied. When designing ATM systems, the common technique is to place controllers on all storeys and to give all controllers identical parameters[14] or to place one controller between the base and first floors. The first method is a very expensive and inefficient method of structural control, while the second method of a single controller does not fully take advantage of the control effectiveness of a multi-controller system. In this paper we will use a gradient based algorithm[15] to optimize the placement and gains of a limited amount of DVFC controllers on buildings. An assumption is that the optimal placement of n controllers is the same as the optimal placement of a single controller added to a system of $n-1$ optimally placed controllers. Thus, each additional controller will optimized one at a time. These buildings with DVFC ATM systems will then be subjected to a simulated earthquake and the maximum and root mean square values of the displacement of the top floor and the control forces will be compared to show the effectiveness of the optimally placed controllers.

EQUATIONS OF MOTION FOR BUILDINGS

The well known equations of motion for a building subjected to an earthquake loading is as follows:

$$\mathbf{M}\ddot{\mathbf{x}}(t) + \mathbf{C}\dot{\mathbf{x}}(t) + \mathbf{K}\mathbf{x}(t) = \mathbf{b}\mathbf{u}(t) + \mathbf{h}w(t) \tag{1}$$

where $\mathbf{M}$, $\mathbf{C}$ and $\mathbf{K}$ are $n \times n$ mass, damping and stiffness matrices and n is the number of floors, u is the control input, w is the ground acceleration (earthquake excitation) and $\mathbf{b}$ is the participation matrix for input control force and $\mathbf{h}$ is the participation matrix for the earthquake acceleration which consists of a vector of floor masses. These equations can be decoupled as modal equations,

$$\mathbf{I}\ddot{\mathbf{q}}(t) + \mathbf{C}_{\mathrm{d}}\dot{\mathbf{q}}(t) + \mathbf{\Lambda}\mathbf{q}(t) = \Phi^{\mathrm{T}}\mathbf{b}\mathbf{u}(t) + \Phi^{\mathrm{T}}\mathbf{h}w(t) \tag{2}$$

and expressed in state space form as

$$\dot{\mathbf{x}}(t) = \mathbf{A}_0\mathbf{x}(t) + \mathbf{B}\mathbf{u}(t) + \mathbf{H}w(t), \quad \mathbf{y}(t) = \mathbf{C}\mathbf{x}(t) \tag{3}$$

where

$$\mathbf{A}_0 = \begin{bmatrix} 0 & \mathbf{I} \\ -\mathbf{\Lambda} & -\mathbf{C}_{\mathrm{d}} \end{bmatrix}, \quad \mathbf{x}(t) = \begin{bmatrix} \mathbf{q}(t) \\ \dot{\mathbf{q}}(t) \end{bmatrix}$$
$$\mathbf{B} = \begin{bmatrix} 0 \\ \Phi^{\mathrm{T}}\mathbf{b} \end{bmatrix}, \quad \mathbf{H} = \begin{bmatrix} 0 \\ \Phi^{\mathrm{T}}\mathbf{h} \end{bmatrix}, \quad \mathbf{C} = [0, \mathbf{c}] \tag{4}$$

In this paper, the tendon controllers are approximated without considering sensor and actuator dynamics. The mass of the tendon controller is also taken to be negligible as compared to the floor mass. For direct velocity feedback control the actuator control force is proportional to the sensor output $\mathbf{y}(t)$:

$$\mathbf{u}(t) = -\mathbf{F}\mathbf{y}(t) \tag{5}$$

GRADIENT-BASED OPTIMIZATION TECHNIQUE

In the following, an optimal design procedure is developed for the actuator placement, $\mathbf{x}_{\mathrm{aj}}$, sensor placement, $\mathbf{x}_{\mathrm{sp}}$, and feedback gains, $\mathbf{F}$. First, a performance function is chosen which includes both the structural response and the control effort. The standard performance function is

$$\hat{J} = \frac{1}{2}\int_0^\infty (\mathbf{x}^{\mathrm{T}}\mathbf{Q}\mathbf{x} + \mathbf{u}^{\mathrm{T}}\mathbf{R}\mathbf{u})\,\mathrm{d}t \tag{6}$$

where $\mathbf{Q}$ and $\mathbf{R}$ are defined as follows:

$$\mathbf{Q} = Q\begin{bmatrix} \mathbf{\Lambda} & 0 \\ 0 & \mathbf{I} \end{bmatrix}, \quad \mathbf{R} = R\begin{bmatrix} \mathbf{I} & 0 \\ 0 & \mathbf{I} \end{bmatrix} \tag{7}$$

The performance function can be expanded in term of the fundamental transition matrix, by substituting for $\mathbf{u}$ as a function of $\mathbf{x}$:

$$\hat{J} = \mathbf{x}^{\mathrm{T}}(0)\left[\frac{1}{2}\int_0^\infty \mathrm{e}^{\mathbf{A}^{\mathrm{T}}t}(\mathbf{Q} + \mathbf{C}^{\mathrm{T}}\mathbf{F}^{\mathrm{T}}\mathbf{R}\mathbf{F}\mathbf{C})\,e^{\mathbf{A}t}\,\mathrm{d}t\right]\mathbf{x}(0) \tag{8}$$

A design procedure which uses this performance function will require discrete values for the initial state, $\mathbf{x}(0)$.[16] Herein, this dependence on $\mathbf{x}(0)$ is eliminated by using a performance function proposed by Levine and Athans.[15] The initial state is modelled as random vector uniformly distributed on the surface of the $2n$-dimensional unit sphere. It has been shown that the average, or expected value of $\hat{J}$, scaled by $2n$, is

$$J = \frac{1}{2}\int_0^\infty \mathrm{tr}\,[\mathrm{e}^{\mathbf{A}^{\mathrm{T}}t}(\mathbf{Q} + \mathbf{C}^{\mathrm{T}}\mathbf{F}^{\mathrm{T}}\mathbf{R}\mathbf{F}\mathbf{C})\mathrm{e}^{\mathbf{A}t}]\,\mathrm{d}t \tag{9}$$

This performance function, which is expressed explicitly in term of actuator and sensor placement vectors, $\mathbf{x}_{\mathrm{aj}}$ and $\mathbf{x}_{\mathrm{sp}}$, (which are imbedded in the matrices $\mathbf{C}$ and $\mathbf{B}$) and the feedback gain matrix, $\mathbf{F}$, is used hereafter.

The optimization problem is

$$\min J(\mathbf{x}_{\mathrm{a}}, \mathbf{x}_{\mathrm{s}}, \mathbf{F}) \to \mathbf{x}_{\mathrm{a}}^*, \mathbf{x}_{\mathrm{s}}^*, \mathbf{F}^*, \tag{10}$$

where J is the cost function, $\mathbf{x}_s$ and $\mathbf{x}_a$ are the placement of sensors and actuators respectively and $\mathbf{F}$ is a feedback gain matrix and $\mathbf{x}_s^*$, $\mathbf{x}_a^*$ and $\mathbf{F}^*$ are the values for the design variables that minimize J. These variables $\mathbf{x}_s$ and $\mathbf{x}_a$ in a continuous case are subject to constraints

$$\mathbf{x}_a \in \mathbf{X}_a, \quad \mathbf{x}_s \in \mathbf{X}_s \tag{11}$$

where $\mathbf{X}_s$ and $\mathbf{X}_a$ are subsets of the domain of the structure, which is limited to the dimensions of the structure.

The derivations of the gradients shown below are previously shown in literature.[15,17] To determine the gradients of the performance function, the following two matrix integrals are needed:

$$\mathbf{K} = \int_0^\infty e^{\mathbf{A}^T t}(\mathbf{Q} + \mathbf{C}^T\mathbf{F}^T\mathbf{RFC})e^{\mathbf{A}t}\,dt \tag{12}$$

and

$$\mathbf{L} = \int_0^\infty e^{\mathbf{A}t}e^{\mathbf{A}^T t}\,dt \tag{13}$$

The matrix $\mathbf{K}$ is related to the performance function by

$$J = \tfrac{1}{2}\,\mathrm{tr}[\mathbf{K}] \tag{14}$$

The matrices can be solved, without numerical integration, by solving the associated Lyapunov equations.[18]

$$\mathbf{KA} + \mathbf{A}^T\mathbf{K} + \mathbf{Q} + \mathbf{C}^T\mathbf{F}^T\mathbf{RFC} = 0 \tag{15}$$

$$\mathbf{LA} + \mathbf{A}^T\mathbf{L} + \mathbf{I} = 0 \tag{16}$$

The Lyapunov equations are efficiently solved by the method of Bartels and Stewart.[19] The control systems used throughout this paper will use single loop collocated sensors and actuators with direct velocity feedback gains. This will eliminate the effect of residual modes causing instabilities in the system.[20] Since the system is collocated, $\mathbf{C} = \mathbf{B}^T$, it is possible to express the gradient of the gain matrix $\mathbf{F}$ as follows:

$$\frac{\partial J}{\partial \mathbf{F}} = -\mathbf{RFCLC}^T + \mathbf{B}^T\mathbf{KLC}^T \tag{17}$$

One of the most robust gradient-based unconstrained optimization techniques is the Davidon-Fletcher-Powell (DFP) algorithm.[21,22] The basic parameters for each iteration are: the vector of optimization variables $\mathbf{X}_i$, an approximate inverse of the Hessian matrix, $\mathbf{H}_i$, and a search direction $\mathbf{S}_i$. After the search direction vector is computed, the one-dimensional minimization proceeds as follows. An accelerated step size algorithm is used to determine an interval in the search direction that contains at least one local minimum. Then, within this interval, cubic interpolation is used to find a minimum. However, if there are more than one local minima in the search direction, convergence may be slow; therefore a combination of cubic interpolation and direct root methods is used. If convergence does not occur after several iterations, then the direct root method is used to reduce the domain so that it includes only one local minimum.

Because earthquakes are random processes, the optimization process will be based on the free vibration response of the system. It has been shown in state control design that the optimal designs for the free vibration system and the random input system are very close.

NUMERICAL EXAMPLE

To get the time domain earthquake response, it is necessary to have a ground acceleration. This can be obtained by using several known earthquake records. Another option is to generate a synthetic earthquake excitation from the power spectral density of an earthquake by using Monte Carlo Simulation.[23] A widely used power spectral density for ground acceleration is

$$\mathbf{\Phi}_{\ddot{\mathbf{x}}_0\ddot{\mathbf{x}}_0}(\omega) = \frac{1 + 4\zeta_g^2\left(\dfrac{\omega}{\omega_g}\right)^2}{\left[1 - \left(\dfrac{\omega}{\omega_g}\right)^2\right]^2 + 4\zeta_g^2\left(\dfrac{\omega}{\omega_g}\right)^2} S^2. \tag{18}$$

Here ζ_g, ω_g and S depend on the characteristics of the ground motion. Thus, the ground acceleration can be expressed as

$$\ddot{X}_g(t) = \psi(t)\ddot{X}_0(t) \tag{19}$$

where $\psi(t)$ is a deterministic envelope function. Using the Fast Fourier Technique, $\ddot{X}_g(t)$ can be represented by a sum,[24]

$$\ddot{X}_g(t) = \psi(t)\sqrt{4\Delta\omega}\ \ \mathrm{Real}\left\{\sum_{k=1}^{M}\left[\sqrt{\Phi(\omega_k)}\mathrm{e}^{\mathrm{i}\alpha_k}\right]\mathrm{e}^{\mathbf{i}\omega_k}\right\} \tag{20}$$

Here α_k are statistically independent random variables uniformly distributed in $(0,2\pi)$; $\omega_k = k\Delta\omega$ in which $\Phi(\omega)$ is evaluated at equally spaced intervals, $\Delta\omega$. In the analysis in this paper the parameters of the earthquake are as follows: $\zeta_g = 0{\cdot}65$, $\omega_g = 18{\cdot}85$ rad/s and $S^2 = 4{\cdot}65 \times 10^{-4}$ m^2/s. The envelope function is defined as follows;

$$\psi(t) = \begin{cases} (t/3)^2 & 0 \leqslant t \leqslant 3 \\ 1 & 3 \leqslant t \leqslant 13 \\ \mathrm{e}^{[-0{\cdot}26(t-13)]} & t > 13 \end{cases} \tag{21}$$

The simulated earthquake ground acceleration is shown in Figure 3.

The output feedback control system consists of m tendon force actuators and collocated sensors located at floor j, where $j = 1, \ldots, n$. The $n \times m$ matrix $\mathbf{b}$ defined in equation (2) is

$$\mathbf{b} = \begin{bmatrix} -1 & 1 & 0 & & \cdots & \\ 0 & -1 & 1 & 0 & & \\ & \vdots & & \ddots & & \\ & & & 0 & -1 & 1 \\ & & \cdots & & 0 & -1 \end{bmatrix} \tag{22}$$

The performance function used is shown in equation (6). **F** is a diagonal $n \times n$ matrix with values F_{ii} = the gain of the controller between the ith and $i-1$ floors. If a controller does not exist between these floors, $F_{ii} = 0$.

The first example structure is an eight-storey structure in which every storey is identically constructed. This example has been used in many numerical studies; it was chosen so the results from this method can be compared to others. The floor mass, m, is 345·6 t; the elastic stiffness of each floor, k, is $3{\cdot}404 \times 10^5$ kN/m; the external damping constant, ß, is 100 kN/m/s; and the internal damping constant, c, is 0. Internal and external damping coefficients are discussed in more depth by Yang.[25] **Q** is chosen to be a diagonal matrix with $Q_{ii} = 13\,000$ for $i = 1, \ldots, 16$. The result for placement of controllers is shown in Figure 2 and Tables I and II.

The second example structure is a 40-storey structure in which every storey is identically constructed. The floor mass, m, is 1290 t; the elastic stiffness of each floor, k, is 10^6 kN/m and the external damping constant, ß, is 100 kN/m/s and the internal damping constant, c, is 0. This active control system was designed using eight modes. **Q** is chosen to be a diagonal matrix with $Q_{ii} = 13\,000$ for $i = 1, \ldots, 8$ and $Q_{ii} = 0$ for $i = 9, \ldots, 16$. Also shown for comparison is the one mode design with $\mathbf{Q}_{11} = 13000$.

PLACEMENT ANALYSIS

Eight-storey building

For the eight-storey structure, the system is designed for four tendon controllers. For structure the tendon controllers are placed below floors 1, 4, 6 and 8. These are shown in Figure 2 and

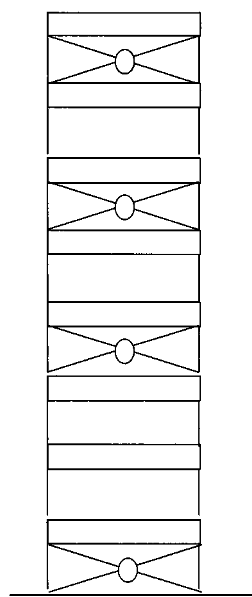

Figure 2. Optimal tendon location for eight-storey structure

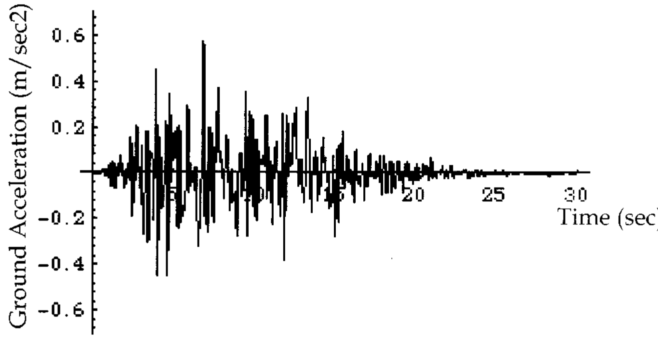

Figure 3. Earthquake excitation

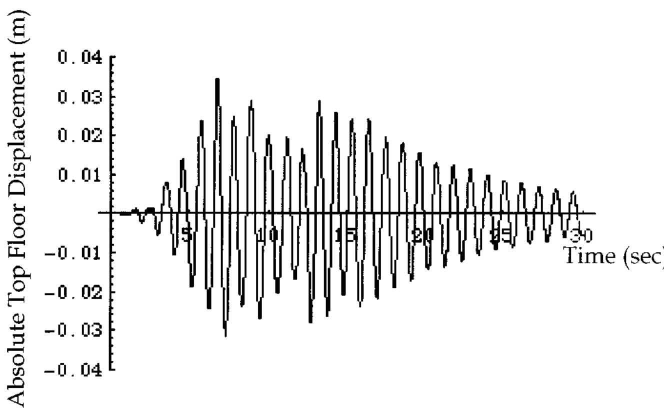

Figure 4. Top floor displacement of eight-storey building (no control)

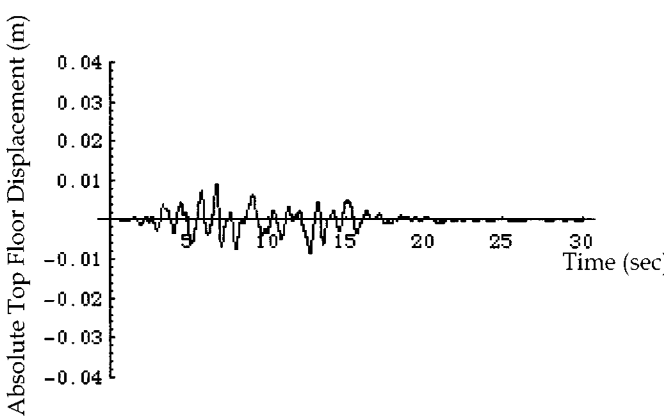

Figure 5. Top floor displacement of eight-storey building (controlled)

Table I. Tendon location for eight-storey building example

Tendon location	1	4	6	8
Gain/m_i (1/s)	35·9	33·6	22·8	39·0
Max force (kN)	201·9	519·6	119·3	75·7
RMS force (kN)	40·4	99·5	21·2	13·5

Table II. Summary of response quantities for the eight-storey building

	No control	Optimal DVFC control	Riccati closed loop
Maximum top floor displacement (cm)	3·47	0·91	1·11
% Reduction in max displacement	—	73·8	68·0%
RMS top floor displacement (cm)	1·25	0·22	0·39
% Reduction in RMS displacement	—	82·4%	68·8%
Maximum control force (10^2 kN)	—	5·20	3·08
Highest RMS control force (10^2 kN)	—	1·00	1·43
Σ Max control force (10^2 kN)	—	10·14	—
Σ RMS control force (10^2 kN)	—	1·73	—

Tables I. What is interesting about this result is that the controller with the highest forces is not the controller under the first floor. Though this has been long thought to be the best condition for the controller on the lowest floor to carry much of the control force, for this system the fourth floor has the highest control forces.

Forty-storey building

For the forty-storey example structure, which is shown in Table III, it seems that in the optimization process, it was deemed that the controller at floor 4 (which was the first found) was to be replaced by a controller at floor 3. As seen in the table, the value for the gain of the controller at floor 4 equals zero. This could represent one of two things. Either the optimization process was not deemed optimal in this case or for the values of $\mathbf{Q}$ and $\mathbf{R}$ specified the maximum number of controllers for this system is nine. Also it is important to note that seven of the 10 controllers are on the lower half of the building and the lowest controller at floor 3 has the largest forces. This shows that for this case the lower floors are more dominant in control.

For the one mode design comparison case, the gains for the systems are nearly identical and the largest forces are produced from the lowest controller located under the first floor. This is because of the smoothness of the performance function for only one mode. This is shown in Table IV.

Table III. Tendon location for forty-storey structure, eight-mode design

Floor location	4	7	11	15	19	24	30	36	3	10
Gain/m_i (1/s)	0·01	1108·0	70·7	1797·0	1442·0	1743·0	1395·0	874·6	2199·0	1864·0
Maximum force (kN)	0·7	4292·0	1063·0	4881·0	4111·0	3438·0	3674·0	2537·0	5175·0	4757·0
RMS force (kN)	0·1	1446·0	303·4	1452·0	1287·0	1091·0	961·5	683·2	1698·0	1508·0

Table IV. Tendon location for forty-storey structure, one-mode design

Floor location	1	2	3	4	5	6	7	8	9	10
Gain/m_i (1/s)	2037·0	2037·0	2036·0	2035·0	2033·0	2028·0	2021·0	2009·0	1993·0	1971·0
Maximum force (kN)	6753·0	6147·0	5809·0	5486·0	5168·0	4848·0	4529·0	4217·0	3923·0	3851·0
RMS force (kN)	1709·0	1632·0	1560·0	1494·0	1435·0	1383·0	1338·0	1301·0	1272·0	1253·0

EARTHQUAKE ANALYSIS

The response quantities examined for all cases were the maximum and the RMS of the absolute top floor displacement and the control forces. The responses for all control forces can be found in the placement tables, while the summary for the eight- and forty-storey buildings can be found in Tables II and V, respectively.

Eight-storey building

Provided are the plots of the maximum control forces for each system. For the eight-storey example this is floor 4 (Figure 6). It is interesting to note again that the controller at the first floor

Table V. Summary of response quantities for the forty-storey building

	No control	Eight-mode design	One-mode design
Maximum top floor displacement (cm)	12·11	10·26	7·14
% Reduction in max displacement	—	15·3%	41·0%
RMS top floor displacement (cm)	5·34	3·55	2·42
% Reduction in RMS displacement	—	33·5%	54·7%
Maximum control force (10^3 kN)	—	5·18	6·75
Highest RMS control force (10^3 kN)	—	1·69	1·71
Σ Max control force (10^3 kN)	—	33·93	50·74
Σ RMS control force (10^3 kN)	—	10·43	14·38

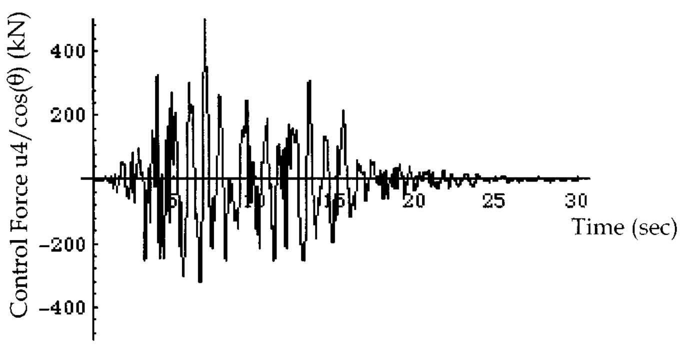

Figure 6. Control force of the 4th floor

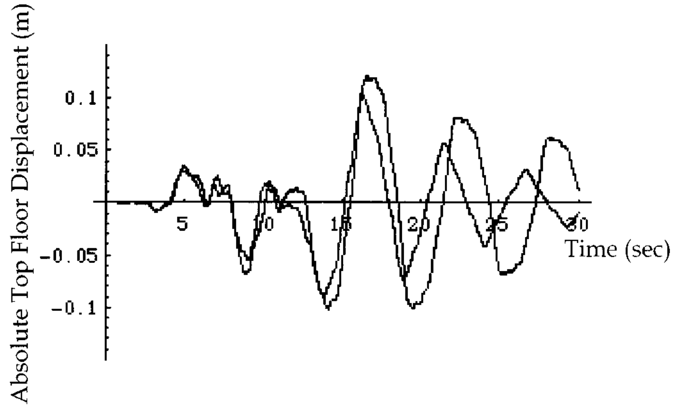

Figure 7. Top floor displacement of forty-storey building (eight mode control)

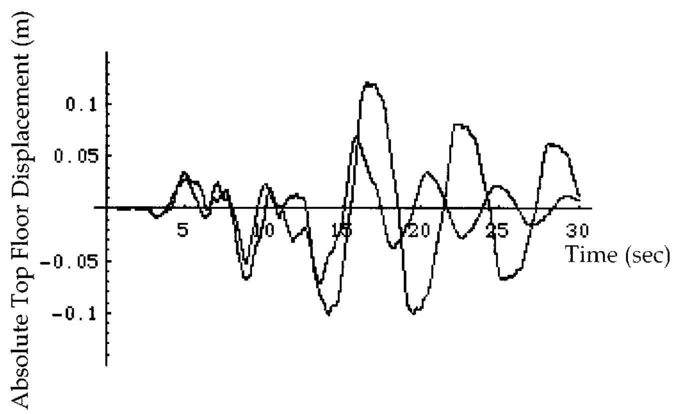

Figure 8. Top floor displacement of forty-storey building (one-mode control)

does not have the largest forces. Though this is probably true for the systems with identical control parameters, it is not safe to assume that the maximum forces will take place under the first floor for any optimal control algorithm. The maximum control force exhibited by any controller is 519·6 kN.

The top floor displacement is as effective as state control response with eight controllers. In Table II, which is a summary analysis for the eight-storey structure, it is shown that the maximum force by a single controller is also in the range of those found for standard Ricatti open-loop control.[26] These results show that optimal (DVFC) can be effective provided the cost function is chosen appropriately.

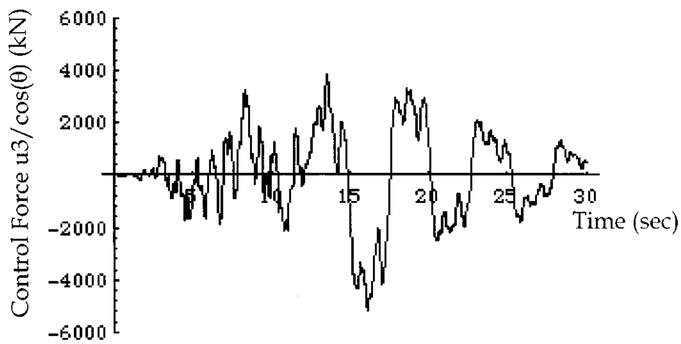

Figure 9. Control force of the 3rd floor for eight-mode design

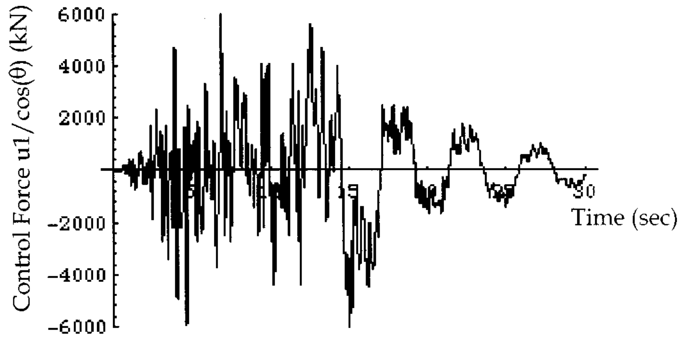

Figure 10. Control force of the 1st floor for one-mode design

Forty-storey building

The performance of the 10 controllers on a forty-storey building is not as effective as that for the eight-storey building. This is to be expected since only 10 controllers were used. The true measure of performance in these cases is the conservation of forces and the RMS response of the top floor displacement. In Table V, it is shown that this control system provides about 15 percent reduction in maximum displacement. This shows the difficulties in designing tall buildings subjected to earthquakes. The control system exhibits a higher amount of damping than the uncontrolled system. This is shown in the more rapid decline of the response, which is shown in Figures 7 and 8, and in the RMS response as shown in Table V.

The system optimized using just one mode, as opposed to the eight-mode design, is much more effective in the control of building response. In this case, the identical control gains make it resemble many of the systems used in design. The one-mode system uses about 30 per cent more RMS control force for about an additional 30 per cent reduction in RMS response. This system also produces much higher maximum control forces than the eight-mode design case.

The plots of the maximum control forces for each case are shown in Figures 9 and 10. In Figure 10, the inability of the one mode system to control the velocity and acceleration is shown in the control force plot of the first floor. This control curve is much choppier and oscillatory than the control plots for the other cases, with the peak early in the loading.

CONCLUSIONS

The proposed optimization technique is very effective in controlling the RMS response of buildings due to earthquakes. It is possible to control the maximum displacement response of the eight-storey building with only 4 controllers. With 10 controllers it is difficult to control the maximum response of A forty-storey building, though there is a significant reduction in RMS response. It is probably possible to control the maximum response, with the addition of more controllers. With similar forces, the DVFC systems provide excellent control for buildings. The control system that rivals that based on full state feedback.[13]

The optimization variables are greatly dependent on the **Q** and **R** matrices. For this reason, it is important that these matrices be chosen with the utmost care.

APPENDIX

Notation

$\mathbf{b}$	participation matrix for input control force
$\mathbf{C}$	damping matrix
$\mathbf{C}_{\mathrm{d}}$	decoupled modal damping matrix
$\mathbf{F}$	time invariant output feedback gain matrix
$\mathbf{h}$	participation matrix for the earthquake acceleration
$\mathbf{I}$	identity matrix
$\mathbf{K}$	stiffness matrix
$\mathbf{M}$	mass matrix
n	number of floors
$\mathbf{Q}$	weight matrix for structural response
$\mathbf{q}$	generalized co-ordinates
$\mathbf{R}$	weight matrix for control forces
t	time
$\mathbf{u}$	control input
$\mathbf{w}$	ground acceleration (earthquake excitation)
$\mathbf{x}$	state variables
$\mathbf{x}_{\mathrm{aj}}$	actuator placement
$\mathbf{x}_{\mathrm{sp}}$	sensor placement
$\mathbf{y}$	vector of sensor outputs
Φ	mode shapes of the structure
Λ	decoupled modal stiffness matrix
ω_{g}	ground motion frequency

$\psi(t)$ deterministic envelope function
ζ_g ground motion damping

REFERENCES

1. L. Meirovitch and L. M. Silverberg, 'Control of structures subjected to seismic excitation', *J. Engng. Mech. ASCE*, **109**(2), 604–618 (1993).
2. T. T Soong, 'Future of active control in civil engineering', *Presentation*, University of Notre Dame (1993).
3. J. C. H. Chang and T. T. Soong, 'Structural control using active tuned mass dampers', *J. Engng. Mech. Div. ASCE* **106**(6), 1091–1098 (1980).
4. A. Kaynia, D. Veneziano and J. M. Biggs, 'Seismic effectiveness of tuned mass dampers', *J. Struct. Div. ASCE* **107**(8), 1465–1483 (1981).
5. E. O. Ayorinde and G. B. Warburton, 'Minimizing structural vibrations with absorbers', *Earthquake Engng. Struct. Dyn.* **8**, 219–236 (1980).
6. Y. Fujino and M. Abe, 'Design formulas for tuned mass dampers based on perturbation technique,' *Earthquake Engng. Struct. Dyn.* **22**(10), 833–854 (1993).
7. M. Abdullah, 'Active control of tall buildings', *Masters Thesis*, Northwestern University, 1991.
8. M. Abe and Y. Fujino, 'Dynamic characterization of multiple tuned mass dampers', *Earthquake Engng. Struct. Dyn.* **23**(8), 813–835 (1994).
9. F. R. Rofooei and I. G. Tadjbakhsh, 'Optimal control of structures with acceleration, velocity and displacement feedback', *J. Engng. Mech. ASCE* **119**(10), 1993–2010 (1993).
10. J. N. Yang and F. Giannopoulos, 'Active tendon control of structures', *J. Engng. Mech. ASCE* **104**(3), 551–568 (1978).
11. B. Samali, J. N. Yang and C. T. Yeh, 'Control of lateral-torsional motion of wind-excited buildings', *J. Engng. Mech. ASCE* **111**(6), 777–796 (1985).
12. L. L. Chung, C. C. Lin and S. Y. Chu, 'Optimal direct output feedback of structural control', *J. Engng. Mech. ASCE* **119**(11), 2157–2173 (1992).
13. M. J. Balas, 'Direct velocity feedback control of large space structures', *J. Guidance Control* **2**(3), 252–253 (1979).
14. J. N. Yang and B. Samali, 'Control of tall buildings in along-wind motion', *J. Struct. Engng. ASCE* **109**(1), 50–68 (1983).
15. W. S. Levine and M. Athans, 'On the determination of the optimal constant output feedback gains for the linear multivariable systems', *IEE Trans. Automat. Control* **AC-15**(1), 44–48 (1970).
16. K. Choe and H. Baruh, 'Actuator placement in structural control', *J. Guidance Control Dyn.* **15**(1), 40–48 (1992).
17. K. Xu, P. Warnitchai and T. Igusa, 'Optimal locations and gains of sensors and actuators for feedback control', *Collection of Technical Papers–AIAA/ASME Structures, Structural Dynamics and Materials Conf.*, Pt.6, 1993, pp. 3137–3145.
18. R. Bellman, *Introduction to Matrix Analysis*, 2nd edn, McGraw-Hill, New York, 1970, p. 174.
19. R. H. Bartels and G. H. Stewart, 'Solution of the matrix equation AX + XB = C', *Commun. ACM* **15**(9), 820–826 (1972).
20. M. J. Balas, 'Trends in large space structure control theory: fondest hopes, wildest dreams', *IEEE Trans. Automat. Control* **AC-27**(3), 522–536 (1982).
21. R. Fletcher and M. J. D. Powell, 'A rapidly convergent descent method for minimization', *Comput. J.* **6**(2), 163–168 (1963).
22. S. S. Rao, *Optimization*; *Theory and Application*, Wiley Eastern Limited, New Delhi, 1978.
23. J. N. Yang and S. C. Liu, 'Distribution of maximum and statistical response spectra', *J. Engng. Mech. ASCE* **107**(6), 1089–1102 (1981).
24. J. N. Yang, 'Simulation of random envelope processes', *J. Sound Vib.* **21**, pp. 73–85 (1972).
25. J. N. Yang, Y. K. Lin and S. Sae-Ung, 'Tall building response to earthquake excitations', *J. Engng. Mech. ASCE*, **106**(4), 801–817 (1980).
26. J. N. Yang, A. Akbarpour and P. Ghaemmaghami, 'New optimal control algorithms for structural control', *J. Engng. Mech. ASCE* **113**(9), 1369–1386 (1987).

